RESEARCH PAPER

Formulation, Optimization of Duloxetine Hydrochloride Loaded Oral Fast Dissolving Films: *In vitro* and *Ex vivo* Evaluation

Monisha S.M.[1,2], Arpitha N. [1,2], Shivakumar H.N[1,2*], Kokila S[3], Rushikesh Shinde[1,2], Yadav V. [1,2], and Yashwanth S[1,2]

[1] *Centre of Innovative Science and Engineering Education, Bengaluru 560010, India.*
[2]*Department of Pharmaceutics, KLE College of Pharmacy, Bengaluru, KLE Academy of Higher Education and Research, Belagavi-590010, Karnataka, India.*
[3]*Department of Pharmaceutics, College of Pharmacy, JSS university, Noida, Uttar Pradesh- 201301*

ABSTRACT

Introduction: Duloxetine hydrochloride (DLX) is a poorly water-soluble antidepressant with low oral bioavailability (~32%) due to acid-mediated degradation in the stomach and extensive first-pass metabolism. Oral fast-dissolving films (ODFs) offer a patient-friendly and effective alternative by promoting rapid drug dissolution in the oral cavity, potentially reducing gastric exposure and improving onset of action. **Materials and Methods:** In this study, DLX-loaded ODFs were prepared by the solvent casting method and optimized using a 14-run D-optimal mixture design. Hydroxypropyl methylcellulose E15 (HPMC E15), maltodextrin (MD), and propylene glycol (PG) were employed as formulation variables to evaluate their influence on film thickness, disintegration time (DT), and percentage drug release at 30 min (Rel_{30}). **Result and discussion:** The prepared films demonstrated uniform physicochemical characteristics, with thickness ranging from 0.24±0.013 to 0.55±0.012 mm, DT from 23±2 to 111±4 s, and Rel_{30} values between 63.30±1.49% and 89.60±1.33%. The optimized formulation (N15), comprising HPMC E15 (109.43 mg), MD (53.23 mg), and PG (637.34 mg), exhibited rapid disintegration (27.61±2.52 s), high drug release (91.18±1.11%), and minimal thickness (0.263±0.013 mm). All formulations showed acceptable content uniformity and near-neutral surface pH. Scanning Electron Microscopy revealed smooth and homogeneous film surfaces, while differential scanning calorimetry and X-ray diffraction confirmed reduced DLX crystallinity within the films. Ex vivo permeation across sheep buccal mucosa resulted in 97.56±7.45 µg/cm² drug permeation within 30 min, indicating partial transmucosal absorption. **Conclusion:** Overall, the optimized DLX-ODFs demonstrated rapid disintegration, enhanced dissolution, and favourable permeation behaviour, suggesting their potential to improve therapeutic onset and reduce first-pass metabolism compared to conventional oral capsules

Keywords: Depression; Duloxetine hydrochloride; Ex vivo studies; Failure Mode and Effect Analysis; Polymeric oral fast-disintegrating films.

How to cite this article: Monisha SM, Arpitha N, Shivakumar HN, Kokila S, Shinde R, Yadav V, Yashwanth S; Formulation, Optimization, and Evaluation of HPMC -Based Oral Fast Dissolving Films Using D-Optimal Design..Int J Drug Deliv Technol. 2026;16(14s): 634-651. DOI: 10.25258/ijddt.16.14s.72

Source of support: Nil.

Conflict of interest: The author declares no conflict of interest, and this work represents independent academic research conducted in a personal capacity, not associated with any employer or commercial entity.

INTRODUCTION

Depression is a prevalent psychiatric disorder that significantly impairs daily functioning and quality of life. [1] Persistent sadness, disinterest in activities, exhaustion, and cognitive decline are its hallmarks. Despite the availability of numerous antidepressant treatments, effectively managing depression remains very challenging. [2,3] Anxiety and depression are the major contributors to the worldwide burden of disease, especially when it comes to years lived with disability, and are linked to substantial morbidity. The development of safe, efficient, and patient-adherent drug delivery systems is necessary due to the chronic nature of many illnesses and the requirement for long-term medication. Inadequate treatment of these conditions not only worsens the suffering of patients but also places an economic burden on society by decreasing productivity and raising healthcare costs. [4,5] Duloxetine hydrochloride (DLX) is a serotonin–norepinephrine reuptake inhibitor (SNRI) indicated for major depressive disorder, generalized anxiety disorder, neuropathic pain, fibromyalgia, chronic musculoskeletal pain, and stress urinary incontinence. The therapeutic action of DLX arises from inhibiting presynaptic reuptake of serotonin and norepinephrine, while elevating prefrontal cortical dopamine by norepinephrine transporter blockade. However, DLX exhibits poor oral bioavailability of 50% as it is acid-labile and prone to extensive first pass metabolism, [6] considering this, DLX is formulated as delayed-release capsules to prevent gastric degradation and therefore attains peak plasma concentrations in ~ 6 hours. Nevertheless, these capsules exhibit delayed onset, inconsistent bioavailability, and are heavily hampered by first-pass metabolism and determined by gastrointestinal transit. Further, patients with dysphagia, particularly those in the elderly, pediatric, and psychiatric groups have difficulties due to the solid oral form. Moreover, there is urgent need to elicit a faster onset of action of DLX in case

**Author for correspondence: shivakumarhn@gmail.com*

of neuropathic pain, fibromyalgia, chronic musculoskeletal pain. However, there are no commercially available orodispersible films in the market that could elicit a faster onset and enhance systemic exposure of DLX. [7] In this context, the present study aims to develop oral fast-dissolving films (ODFs) considering the gastric degradation and extensive first-pass metabolism of DLX. Embedding DLX within a hydrophilic polymer matrix is anticipated to improve wettability, reduce crystallinity, and promote faster drug dissolution. The dissolved drug is likely to be absorbed from the oral cavity that would evade the acid degradation and the first pass metabolism to improve the bioavailability. [8] In this context, we plan to employ a mixture design to systematically evaluate the effect of polymer, co-former, and plasticizer levels proportions in the casting solution on critical quality attributes (CQAs) of the ODFs such as film thickness, disintegration time (DT), and percentage drug release at 30 min. (Rel_{30}). Further, we plan to optimize the composition of the casting solution using desirability-based numerical approach to obtain ODFs that would undergo rapid disintegration and elicit prompt availability of DLX in the oral cavity. Such rapid release may facilitate transmucosal absorption, thereby reducing the gastric degradation and first-pass losses enabling a faster therapeutic onset. The faster onset of action would be the need-of-hour in management of pain and CNS disorders. [9] To the best of our knowledge, this work represents the first-of-its kind comprehensive attempts to develop and statistically optimize DLX-loaded ODFs that would address both solubility issues and metabolic constraints associated with the conventional oral dosage forms. Thus, the study, which involves the development of DLX-loaded ODFs, is novel and unique as such a study has not been previously reported.

MATERIALS AND METHODS

Materials

DLX was a gift sample from Dr. Reddy's Laboratories, Hyderabad, India. Hydroxypropyl methylcellulose E15 (HPMC E15) was purchased from CDH Fine Chemical, New Delhi, India. Maltodextrin (MD) and Propylene Glycol (PG) were purchased from SD Fine Chemical, Mumbai, India. Potassium dihydrogen phosphate was purchased from Molychem Ltd, Mumbai, India. Sodium hydrochloride, citric acid, and mannitol was purchased from Spectrum Reagents and Chemicals Pvt. Ltd., Coimbatore, Tamil Nadu, India. Dialysis Membrane (12,000 MWCO) was purchased from Himedia Laboratories Pvt. Ltd, Maharashtra, India.

Determination of melting point

The melting point of DLX was determined using the capillary tube method. A pre-defined quantity of the sample was packed into a capillary tube and inserted into the melting point analyzer (DBK Prog. Melting Point Apparatus, Mumbai, India). The instrument is then used to observe the physical transition from solid to liquid. The temperature at which the substance fully melts is recorded as the melting point.[10]

Preparation of DLX-ODFs

A D-optimal mixture design was employed in Design-Expert® to optimise DLX-loaded oral fast-dissolving films (ODFs) by film casting technique to understand the effect of key formulation components influencing the key quality attributes. In line with the QbD principles, Failure Mode and Effects Analysis (FMEA) was used before hand to identify high-risk components, that could compromise film integrity, disintegration, or mechanical strength **Table 1 & Figure 1**. This allowed early-risk prioritisation and informed control-strategy development. A set of preliminary investigations indicated that three components, namely proportion of HPMC E15, MD, and PG that were varied across two levels as indicated **Table 2**.

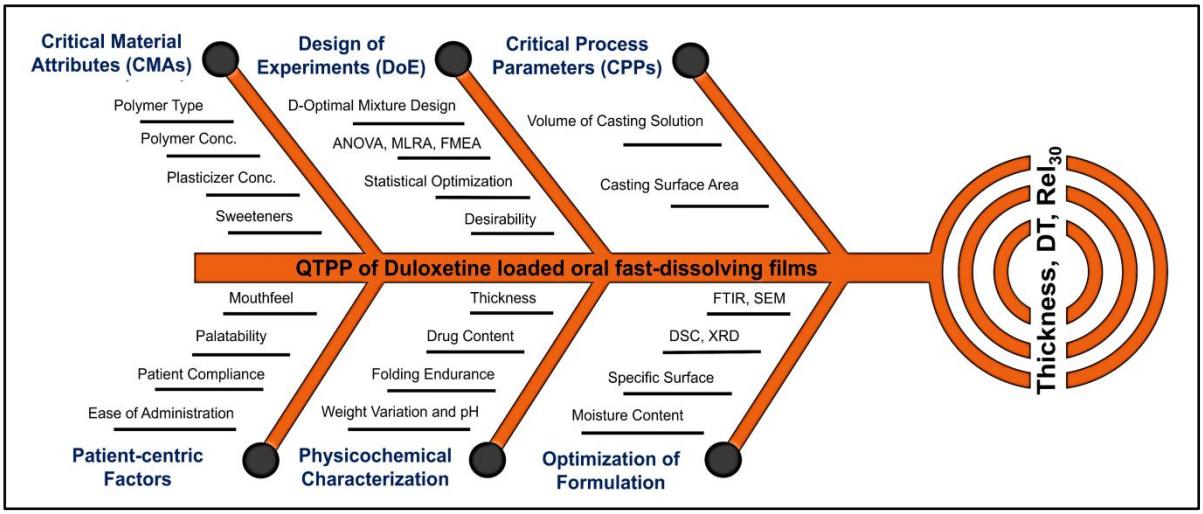

Figure 1. Failure mode and effect analysis (FMEA) illustrating risk analysis for the development of a Duloxetine Oral Fast Dissolving Film.

Fourteen formulations, including replicates, were generated to explore synergistic, antagonistic, and nonlinear interactions. Disintegration time, thickness, and Rel_{30} served as responses reflecting patient acceptability and product consistency. ODFs were prepared by the solvent casting technique, wherein the polymers and plasticizer were dissolved in water at 10000 rpm for 5min, then DLX incorporated, and the mixture homogenised (IKA®, T18 Digital Ultra Turrax®, IKA-Werke GmbH & Co. KG, Baden-Wurttemberg, Germany) for 5 min and sonication (Labman Scientific Instruments Pvt. Ltd., Chennai, India) **Table 3**. The degassed solution was cast onto pre-plasticised Petri dish (12.56 cm^2), dried at room temperature and then at 40±2°C for 48h. Dried films were peeled, cut into 1×1 cm^2 pieces, and stored in airtight containers **Figure 2**. Overall, integrating principles of FMEA with a DoE reduced experimentation, enhanced process understanding, and enabled reliable optimisation of film composition and performance.[11]

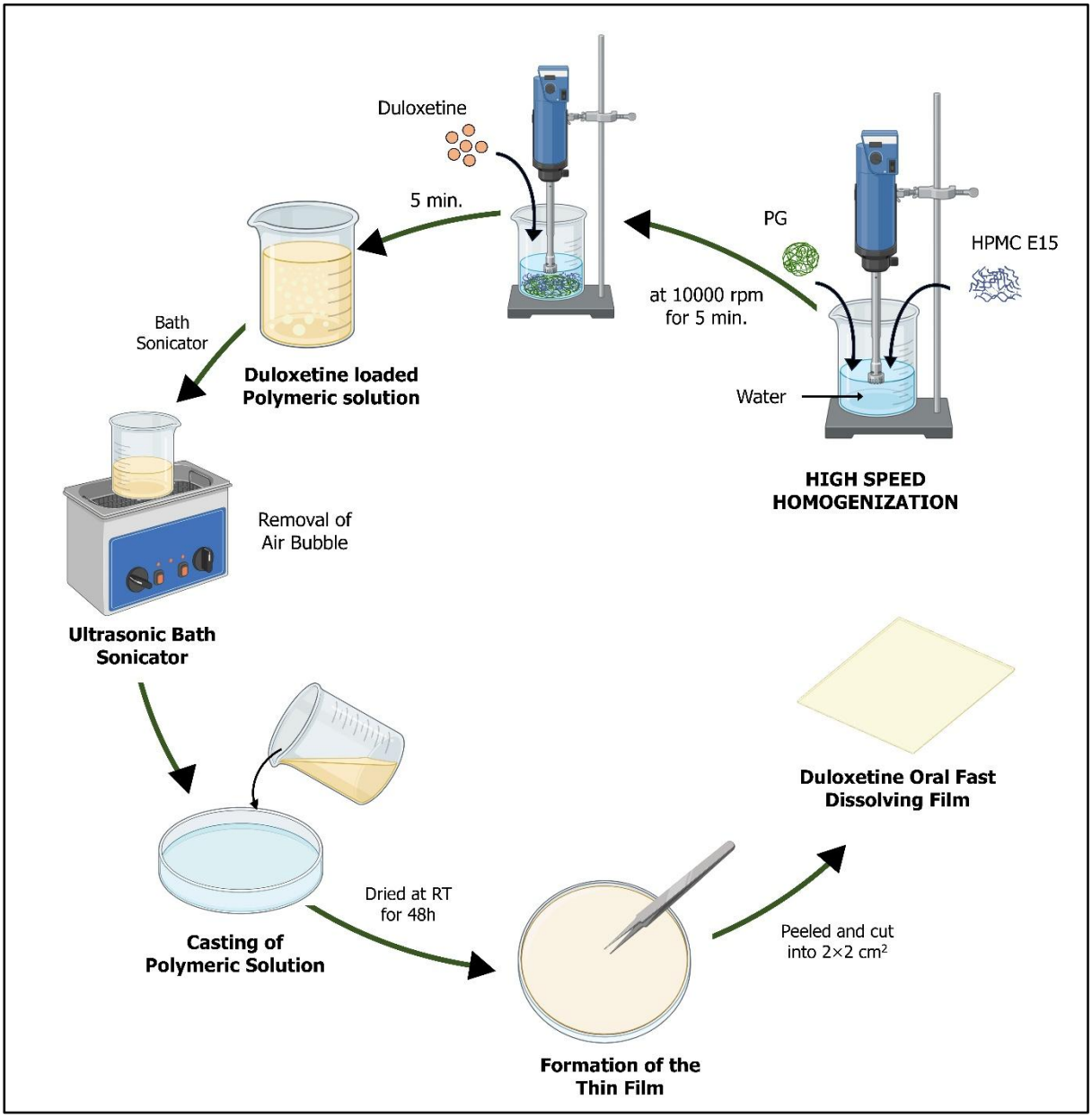

Figure 2. Schematic representation of the steps involved in preparation of duloxetine oral fast-dissolving films by solvent casting technique.

Table 1. Quality Target Product Profile for Oral Fast-Dissolving Films of Duloxetine Hydrochloride

QTPP Elements	Target	Justification
Dosage Form	Oral films	Designed for rapid disintegration and onset of action, resulting in improved bioavailability and therapeutic effectiveness
Route of Administration	Oral	Most patient-friendly and widely accepted route
Drug Product Quality Attributes		
Disintegration Time (secs)	Minimize	Enables faster drug release, most likely facilitates quicker onset of action, and improved patient acceptability, in patients with swallowing difficulties.
Thickness (mm)	Minimize	Reduces the DT, improves flexibility while supporting consistent mechanical strength.
Drug Release at 30 min (Rel_{30})	Maximize	Enables quicker drug absorption, rapid systemic availability which improves neuropathic conditions with quick dissolution shortens DT.

Table 2. Independent and dependent variables as per D-optimal mixture design

Independent variables	Low level (-1)	High level (+1)
A: HPMC[a] E15 (mg)	100	250
B: MD[b](mg)	50	150
C: PG[c] (mg)	425	650
Dependent variables	**Constraints**	
Y_1: Thickness (mm)	Minimize	
Y_2: DT[d] (sec.)	Minimize	
Y_3: Rel_{30}[e] (%)	Maximize	

[a]Hydroxylpropyl methylcellulose, [b]Maltodextrin, [c]Propylene Glycol, [d]Disintegration time and [e]Percentage drug release at 30 min.

Table 3. Formulation batches based on D-Optimal Design

Runs	HPMC[a]E15 (mg)	MD[b](mg)	PG[c] (mg)
N1	148.36	150	501.63
N2	207.50	100.32	492.16
N3	205.82	50	544.17
N4	250	50	500
N5	100	50	650
N6	250	125	425
N7	162.99	95.99	541
N8	198.91	150	451.09
N9	100	150	550
N10	154.56	50	595.43
N11	100	101.33	598.66
N12	100	50	650
N13	250	125	425
N14	250	50	500

[a]Hydroxylpropyl methylcellulose, [b]Maltodextrin, [c]Propylene Glycol. The total weight of the solid content in each run was 800mg in 10mL casting solution.

Regression analysis

D-optimal mixture design was employed to assess the effects of HPMC E15 (A), MD (B), and PG (C) on the thickness, Rel_{30}, and disintegration time of DLX-ODFs. ANOVA showed significant quadratic model terms ($p<0.05$), separating composition effects from experimental error. All responses were described by second-order polynomial mixture equation,

$$Y = \beta_1 A + \beta_2 B + \beta_3 C + \beta_{12} AB + \beta_{13} AC + \beta_{23} BC$$

Where, Y is the response (thickness, DT, and Rel_{30}), A, B, and C are the proportions of HPMC E15, MD, and PG, respectively, β_1, β_2, and β_3 are the regression coefficients representing the main effect of each component. Likewise, β_{12}, β_{13}, and β_{23} are the coefficients representing two-way interactions between components, enabling evaluation of both main effects and interactions. Model adequacy was supported by high R^2 values, matched adjusted–predicted R^2, minimal lack-of-fit, and adequate precision, indicating strong predictive performance for formulation optimization.

Optimization of the composition and validation of the mathematical models

The mathematical models were validated by developing an optimized formulation with the most desirable quality attributes to ensure a pulsatile release. Constraints were set on the responses to identify optimal composition, focusing on minimizing thickness and DT to maximize Rel_{30}. The optimized ODFs were evaluated for these quality attributes, and experimental results were compared with those predicted to assess the prediction error. A lower prediction error would indicate the accuracy and reliability of the generated mathematical models.

Evaluation of Duloxetine Oral Fast-dissolving Films

Compatibility studies

Fourier transform infrared (FTIR) spectroscopy was recorded using a FTIR spectrophotometer (Jasco FTIR, 460PLUS spectrometer, Tokyo, Japan) and was employed to characterize DLX and to evaluate drug–excipient compatibility. Pure DLX was mixed with KBr and scanned over 4000–400 cm^{-1} to identify characteristic functional groups.[12] Infrared spectra of DLX, individual polymers, the physical blend, and the optimized formulation were compared for shifts or changes to detect drug-excipient interactions. [13,14]

Weight uniformity

Weight uniformity of ODFs was assessed by individually weighing pre-cut sections (1×1cm^2) obtained from three different areas of each batch using a calibrated analytical balance (Shimadzu BL-220H, Kyoto, Japan). The mean weight, SD, and the percentage deviation was determined to evaluate consistency, with all films were required to remain within ±5% deviation of the mean weight. [15]

Folding endurance (FE)

Mechanical durability of the DLX-ODFs was determined by repeatedly folding films until breakage; folding endurance was the number of folds before failure, assessed in triplicate. The results are presented as the mean±SD. [16]

Surface pH measurement

Surface pH of prepared films was measured after equilibration with a simulated salivary fluid (SSF) of pH 6.8 for 30s. The pH electrode (Lab Junction, LJ-131, Panchkula, India) was placed in direct contact with the film surface for a duration of 1 min. Measurement were performed in triplicate and reported as mean±SD. [17,18]

Drug content

A 1×1 cm^2 section of the film was dissolved in water in a volumetric flask to evaluate the DLX content. The resulting solution was then diluted with phosphate buffer (pH 6.8). The absorbance of the diluted sample was measured using a UV-visible spectrophotometer (Shimadzu UV-1900i, Kyoto, Japan), [19] and the assay was determined using a standard calibration curve created in the same solvent system. The analyses were performed in triplicate, and the results are presented as mean±SD.

Tack test

Tackiness refers to the degree of stickiness or adhesive potential of the ODFs that can be assessed under both dry and semi-moist conditions. Bio-adhesive films are typically characterized by a high degree of surface adhesion, which contributes to their effectiveness in transmucosal drug delivery. In this study, tackiness was qualitatively evaluated by manually applying pressure to the film surface using the thumb. Each formulation was tested in triplicate, and results were reported based on consistent tactile observations to ensure repeatability. [20]

Thickness measurement

The thickness of ODFs was measured to assess uniformity across the casted samples. For each formulation were randomly chosen at three different regions, and thickness measurements were taken at five distinct points (centre and edges) using a digital calliper (Mitutoyo 500- 196-30, Kawasaki, Japan), accurate to 0.01 mm. Measurements were conducted in triplicate for each sample, and results were reported as the mean±SD. [21]

Moisture content

Moisture content in prepared films was scientifically evaluated by determining the percentage decrease in weight after exposure to desiccation. Accurately weighed film samples were placed in a desiccator containing anhydrous calcium chloride as the desiccant and maintained under controlled dry conditions for duration of three days. Upon completion of the desiccation period, films were reweighed, and the percentage of moisture loss was calculated using the following equation:

$$\mathbf{MC}\ (\%) = \frac{(\mathrm{Wi} - \mathrm{Wf})}{\mathrm{Wi}} \times 100$$

where′Wi′is the initial weight and ′Wf' is the final weight of the film. [22] The moisture content determined in triplicate for each formulation and results are expressed as mean ±SD.

Disintegration time (DT)

The ability of oral films to disintegrate rapidly is essential for the immediate release of the incorporated drug. To evaluate DT, randomly selected film samples (1×1cm^2) were subjected to testing using a USP disintegration apparatus (Electrolab, ED-2, Mumbai, India) filled with 900mL of water maintained at 37±2°C. The time required for complete disintegration of each film sample was recorded. Each formulation was tested in six replicates, and the results were expressed as mean ± standard deviation. [23]

***In vitro* drug release**

In vitro drug release from DLX ODFs was evaluated using the USP dissolution apparatus type V (ElectrolabTDT-08T, Mumbai, India). Films mounted on stainless steel discs were placed in 500

mL of simulated salivary fluid (pH 6.8) at 37±0.5°C, under the paddle rotating at 50 rpm. At specified intervals, samples were withdrawn, filtered (0.45 µm), and replaced with pre-warmed medium to maintain sink conditions. Samples were diluted and analysed using a UV-visible spectrophotometer. Rel_{30} was quantified using a standard calibration curve, and results were reported in triplicate. [24] Further, the percentage dissolution efficiency (%DE) was calculated based on the area under the curve equation. Higher values of %DE indicate the potential of the formulation to generate a pulsatile drug release.

$$\mathbf{DE}(\%) = \frac{\int_{t0}^{T} y_t(dt)}{y_{100} \times T} \times 100$$

Where 't_0' is the initial and 'T' is the final time point of the dissolution study, 'y_t' is the percentage of drug dissolved at any time 't', and 'y_{100}' is 100% dissolution.

Kinetic models with release mechanism

Attempts were made to fit the dissolution data for the DLX, and DLX-loaded films to a first-order model to elucidate the drug release kinetics was followed by this equation. [25]

$$Q_t = Q_0 e^{-\mathbf{k_1}t}$$

Where 'Q_0' and 'Q_t' indicate the drug release levels at specific time intervals '0' and at time 't' respectively while 'K_1' is the first-order rate constant.

The dissolution data were analyzed by fitting into Hixson-Crowell's mathematical model, which describes the drug release from systems with changes in surface area as well as the diameters of particles. It is calculated by the cube of the drug's remaining matrix fraction displaced versus time. [26]

$$\sqrt[3]{W_0} - \sqrt[3]{W_t} = \mathbf{k_{HC}}t$$

Where '$\sqrt[3]{W_0}$' is the initial amount of drug, '$\sqrt[3]{W_t}$' is the weight of DLX at time 't', 'K_{HC}' is the Hixon and Crowell's release constant.

Scanning Electron Microscopy (SEM)

SEM was performed to investigate the surface topography of the polymer matrix. Film specimens from the optimized batch N15 were sputter-coated with gold and analysed under SEM (EVO MA18, Oxford EDS, X-act, Oberkochen, Germany) at various magnifications. The photograph was taken at 8K resolution with an accelerating voltage of 10–15 kV. Attention was given to the polymer surface morphology. [27]

Differential Scanning Calorimetry (DSC)

The thermal behaviour of DLX, their physical mixture, and the optimized formulation N15 was investigated using Differential Scanning Calorimetry (DSC-60-Shimadzu, Kyoto, Japan). Approximately 5–10 mg of each sample was placed in a sealed aluminium pan and heated from 120 to 240°C at a rate of 10°C/min under a nitrogen purge to maintain an inert atmosphere. [28] The degree of crystallinity (Xc) of the sample film was computed using DLX as reference, using equation. [29]

$$\mathbf{Xc} = \frac{\Delta Hm}{(1-w).\Delta H°m} \times 100$$

Where 'ΔHm' represents the measured heat of fusion, '$\Delta H°m$' is the heat of fusion for 100% crystalline DLX, and 'w' is the weight fraction of the sample within the carrier matrix.

X-ray diffraction (XRD)

The crystalline characteristics of DLX and its formulations were examined using a Rigaku Miniflex 600 (Tokyo, Japan) Powder X-ray Diffractometer. The analysis employed Cu-Kα radiation (λ=1.5406Å) as the X-ray source, operating at an accelerating voltage of 40 kV and a current of 15 mA. X-ray diffraction patterns were recorded across an appropriate 2θ range of 5° to 40°, with a scan rate of 0.5sec per step, and a fixed working distance of 10mm. The degree of crystallinity (DOC) was quantitatively assessed using equation:

$$\mathbf{DOC}\ (\%) = \frac{Is}{Ir} \times 100$$

where 'I_s' is the intensity of the most prominent diffraction peak of the sample, 'I_r' is the intensity of a standard reference peak at a similar angle. This evaluation enabled the determination of relative crystallinity. Sharp and well-defined peaks in the diffractogram represent a high degree of crystallinity, while the absence or broadening of peaks in the film samples suggested partial or complete amorphization. [30,31]

***Ex vivo* mucoadhesion strength studies**

Mucoadhesive strength of the optimized film was determined using a modified two-arm balance technique, as described in established literature. Freshly excised sheep buccal mucosa served as the biological substrate. A 2 mm-thick section of the mucosa was rinsed with phosphate-buffered saline, conditioned with simulated saliva, and fixed to a metal platform. A 1×1 cm^2 film was attached to the balance pan, contacted with the mucosa for two minutes, and the detachment force was measured by adding weights until separation. [32]

***Ex vivo* permeation studies**

Ex vivo permeation study was conducted using a Franz diffusion cell (Orchid Scientific, India). Freshly excised sheep oral mucosa was mounted between the donor and receptor compartments. The optimized film was secured on the donor side, while phosphate buffer (pH 6.8, 5mL) filled the receptor compartment. For solution permeation, 0.5mL of drug solution was placed in the donor compartment. The receptor medium was maintained at 37±2°C and stirred continuously at ~600rpm with a magnetic stirrer to simulate physiological conditions. At predetermined intervals over 30 min., samples (1mL) were withdrawn from the receptor

compartment, filtered through a 0.45 µm membrane filter, and analysed for drug content using a UV-visible spectroscopy, and replaced with fresh buffer. Data were expressed as the mean of three independent experiments. [33]

Statistical analysis

The data were analyzed using Analysis of Variance (ANOVA) facilitated by the Design Expert®13, Stat-Ease, Inc., Minneapolis, MN, USA. Statistical significance was determined at a probability threshold of $p < 0.05$. The experimental data generated were computed using GraphPad Prism 5 (GraphPad, San Diego, CA, USA). Standard deviation is represented by error bars in all graphs to ensure an accurate and consistent interpretation of data variability.

RESULTS AND DISCUSSION

Melting point of DLX

The thermal transition of pure DLX was evaluated in triplicate using a programmed melting apparatus, yielding a result of 170.50±2.5°C. This value aligns with established literature data, [34] thereby affirming the drug's purity and identity.

Preparation of duloxetine loaded oral fast-dissolving films

The D-optimal mixture design was applied to develop and optimize DLX loaded ODFs by assessing the effects of HPMC E15 (**A**), MD (**B**), and PG (**C**) on DT (Y_1), thickness (Y_2), and Rel_{30} (Y_3). The fourteen formulations, including replicates, were found to be non-tacky and displayed uniform thickness, consistent drug content, and acceptable surface pH. HPMC E15, a hydrophilic, film-forming polymer, which slows water penetration and prolong DT, while MD as hydrophilic, fast-dissolving carbohydrate, accelerates wetting and enhances solubilization, whereas PG, a plasticizer, improves flexibility, supports drug diffusion and release. This statistical approach successfully enabled identification of optimal composition of the casting solution to obtain ODFs that display quick disintegration time and rapid dissolution [35].

EVALUATION OF ORAL FAST-DISSOLVING FILM OF DULOXETINE

Weight variation

The average weight of the developed ODFs (1×1 cm^2) ranged between 26.00±0.02 and 71.00±0.01 mg **Table 4**. The observed variation in weights across formulations can be attributed primarily to the differences in concentrations of HPMC E15, PG, and MD used in the casting solutions. Higher concentrations of HPMC E15 and PG generally increased the solid content, leading to thicker films, as seen in runs such as N6 (71.00±0.01mg). Conversely, formulations with lower polymer concentrations tend to produce lighter films, like N5 (26.00±0.02 mg). The amount of polymers and PG were found to be the major contributors to the weight. Achieving uniformity in film weight is crucial to ensure dosage accuracy, and the solvent casting technique was found to ensure dose precision, as reflected in the consistent weights obtained across the batches. [36]

Folding endurance (FE)

FE of films prepared with HPMC E15, MD, and PG depends critically on the interplay of their functions, ranging from 253±1 to 376±6. HPMC E15 serves as the film-forming polymer providing structural strength and cohesive integrity. [37] MD, used as a matrix-forming (or co-polymer) component, helps improve film uniformity, reduce brittleness, and modify the mechanical profile, imparting better flexibility. [38] PG, as a plasticizer, lowers the glass transition temperature of the polymers, increases molecular mobility, and enhances elasticity, thereby reducing brittleness and preventing micro-cracks on repeated folding **Table 4**. Formulations with insufficient PG were brittle and displayed low folding endurance, while those with optimized HPMC E15, MD, and PG yield films with good flexibility and mechanical strength. [39,40]

Table 4. Physicochemical Parameters of Duloxetine Oral Fast-Dissolving Films

Run	Thickness (mm)	WV[a] (mg)	DT[b] (sec.)	Surface pH	FE[c]	DC[d] (%)	MC[e]	Rel_{30}[f] (%)
N1	0.41± 0.012	40.27±0.04	76.00±2	6.47±0.06	292±2	89.34±1.12	1.79±0.03	69.12±1.29
N2	0.48±0.010	49.64±0.02	95.00±3	6.47±0.12	271±4	90.29±1.38	1.26±0.05	73.71±1.20
N3	0.39±0.010	32.09±0.01	66.95±4	6.83±0.06	318±2	92.68±1.65	1.07±0.02	83.02±1.37
N4	0.44±0.012	40.33±0.04	89.00±3	6.57±0.21	289±5	88.47±1.62	1.68±0.06	81.03±1.43
N5	0.24±0.013	26.00±0.02	23.00±2	6.80±0.10	376±3	96.01±1.38	1.01±0.03	89.60±1.33

N6	0.55±0.011	71.00±0.01	111.00±4	6.70±0.10	253±2	88.73±1.36	2.12±0.04	84.72±1.50
N7	0.41±0.013	37.52±0.02	67.00±3	6.47±0.06	301±4	90.55±1.38	1.45±0.04	72.10±1.49
N8	0.51±0.004	59.34±0.01	104.00±2	6.53±0.06	262±2	89.76±1.59	1.95±0.05	72.40±1.44
N9	0.30±0.012	28.27±0.04	47.00±4	6.50±0.10	332±1	93.11±1.65	1.53±0.02	77.69±1.39
N10	0.32±0.014	27.67±0.02	44.63±3	6.87±0.06	346±3	94.10±1.12	1.13±0.04	86.34±1.32
N11	0.28±0.010	27.33±0.01	35.73±4	6.47±0.06	359±4	95.02±1.36	1.31±0.03	65.40±1.40
N12	0.24±0.015	26.00±0.03	23.00±3	6.82±0.10	376±6	96.01±1.62	1.01±0.03	89.42±1.32
N13	0.55±0.012	71.00±0.01	111.00±4	6.68±0.10	253±1	88.73±1.38	2.12±0.04	83.50±1.43
N14	0.44±0.010	40.33±0.04	89.00±2	6.57±0.21	289±5	88.47±1.12	1.68±0.06	63.30±1.49

[a]Weight Variation, [b]Disintegration time, [c]Folding Endurance, [d]Drug Content, [e]Moisture content, [f]Drug release at the end on 30 min. All values in the table are expressed as mean±SD (n=3).

Surface pH measurement

The surface pH of the developed ODFs ranged from 6.47±0.06 to 6.83±0.06, indicating good mucosal compatibility and minimal irritation potential **Table 4.** [41] Although polymeric films may possess a slightly acidic internal environment, the measured surface pH supported patient comfort and acceptable tolerability. [42] Maintaining a near-neutral pH also promotes drug stability and favorable interaction with saliva. [43] The consistent pH across formulations reflects the suitability of the selected excipients, HPMC E15 as the film-forming polymer and MD as the matrix material, both recognized for their safety and compatibility in oral film systems. [44]

Drug content

The developed ODFs exhibited consistent drug content (88.47 ± 1.12–96.01 ± 1.62%), demonstrating the reliability of the solvent-casting method. Uniformity is attributed to the film-forming property of HPMC E15, [45] which ensures homogeneous drug distribution, and the matrix-forming effect of maltodextrin, which stabilizes the film structure. These results confirm that the polymer–matrix system and method provide a robust, scalable platform for ODF development **Table 4** [46].

Tack test

Formulations were found to be non-tacky, indicating that the films were adequately dried during the manufacturing process. The non-tacky nature of the polymeric films is generally associated with proper solvent evaporation and film stability. Moreover, non-tacky films are typically indicative of a well-formed matrix, which often ensures faster disintegration upon administration in the oromucosal cavity due to minimal surface adhesion and rapid hydration. [47]

Moisture content

The MC analysis of the DLX-ODFs formulations demonstrated values ranging from 1.01±0.03 to 2.12±0.04%. This narrow range reflects consistent moisture retention across the formulations, indicating proper control during the drying and storage processes. [48] Adequate moisture content is a critical parameter for oral film systems, as it ensures sufficient flexibility to prevent brittleness while maintaining structural stability **Table 4**. Moreover, controlled moisture levels help preserve the films' mechanical strength and contribute to their microbial safety. [49] Overall, the observed moisture content range supports the suitability of the prepared formulations for handling, packaging, and long-term stability.

Impact of independent variables on dependent variables

Impact on thickness

ANOVA for film thickness revealed that the quadratic model was highly significant, with an F-value of 917.10, with a $p < 0.0001$. The model demonstrated excellent fit, with $R^2 = 0.9983$, Adjusted $R^2 = 0.9972$, and Predicted $R^2 = 0.9952$. The adequate precision was 85.45, indicating a strong signal-to-noise ratio, and the lack-of-fit was non-significant ($p>0.05$), confirming the validity of the model. Regression equation (coded factors) was:

$$\mathbf{Y1} = 0.4653 \cdot \mathrm{A} + 0.2036 \cdot \mathrm{B} + 0.2365 \cdot \mathrm{C} + 0.9081 \cdot \mathrm{AB} + 0.2646 \cdot \mathrm{AC} + 0.3412 \cdot \mathrm{BC}$$

Among the individual components, HPMC E15 (A) had the most substantial influence on film thickness. The higher viscosity and film-forming ability of HPMC E15 contributed to the production of thicker films. MD (B) and PG (C) contributed to the

thickness to a lesser extent but played important roles in maintaining matrix structural integrity. The interaction between HPMC E15 and MD (AB) had the highest coefficient (0.9081), indicating a strong synergistic effect on thickness. This suggests that when both polymers are used in optimal proportions, they reinforce the structural density of the film. The AC and BC interactions also displayed statistically significant contributions, highlighting that the plasticizer interacts differently with each polymer and influences film-forming capacity and crosslinking behavior. Contour and 3D surface plots (**Figure 3**) indicated that film thickness increased with rising HPMC E15 and PG levels. Regions with higher HPMC E15 proportions were associated with the thickest films. These visual depictions confirmed that thickness is primarily governed by the polymer-to-plasticizer ratio.

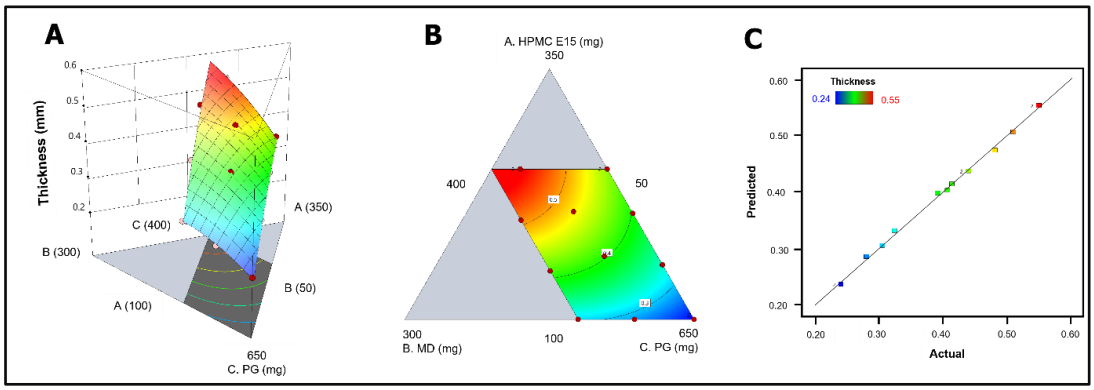

Figure 3. Three-dimensional surface plots (A), Two-dimensional contour plots (B), and Correlation plots of actual versus predicted values (C) depicting the interactive effects of independent variables on the thickness of films. The plots are color-coded, with blue indicating lower values while red indicating higher response values.

Impact on disintegration time

DT is found to be the rate determining step in drug dissolution and the drug release. The quadratic model for DT was significant with F =173.93 and p < 0.0001. The model fit indices were R^2 = 0.9909, Adjusted R^2 = 0.9852, and Predicted R^2 = 0.9749. Adequate precision was 37.25 and lack-of-fit was insignificant in the equation. The regression model (coded form) was:

$$\mathbf{Y2} = 113.01 \cdot A + 73.67 \cdot B + 21.18 \cdot C + 102.05 \cdot AB + 44.77 \cdot AC + 26.97 \cdot BC$$

HPMC E15 had the largest positive impact as it prolonged the disintegration time. As a hydrophobic, film-forming polymer, HPMC E15 delayed water penetration and prolonged film disintegration. The trends suggest that simultaneous increases in HPMC E15 with either MD or PG may lead to prolonged disintegration, highlighting potential antagonism between hydrophobic and hydrophilic components. Contour plots demonstrated that disintegration time decreased in regions with high PG and MD, especially when HPMC E15 levels were minimized. The 3D surface plots confirmed that optimal rapid disintegration occurred in formulations with high plasticizer content. These plots were critical for visually defining regions of rapid film breakdown suitable for oromucosal delivery (**Figure 4**).

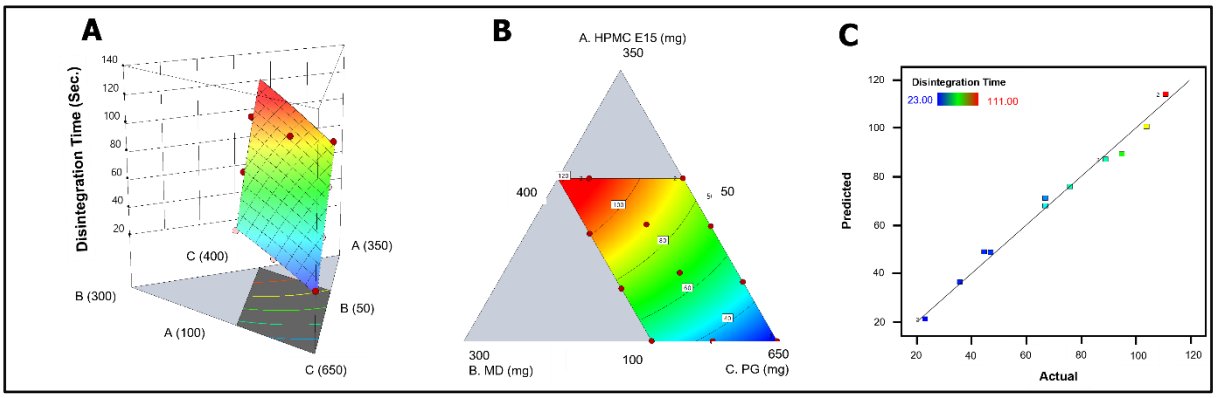

Figure 4. Three-dimensional surface plots (A), Two-dimensional contour plots (B), and Correlation plots of actual versus predicted values (C) depicting the interactive effects of independent variables on the disintegration time of films. The plots are color-coded, with blue indicating lower values while red indicating higher response values.

Impact on *in vitro* drug release

Rel_{30} that denotes the percentage of drug release at the end of 30 min is a key indicator of the onset of action in ODFs. Higher Rel_{30} values reflect faster film dissolution and drug availability for absorption, which are essential for rapid therapeutic response in acute conditions. [50] Rel_{30} ranged from 63.30±1.49% to 89.60±1.33% within 30 min (**Table 4)**, with higher plasticizer levels promoting film erosion, enabling fast, quicker release that would likely improve drug absorption.

The model for Rel_{30} was found to be statistically significant ($F = 12.21$, $p<0.0021$), with excellent model fit indices: $R^2 = 0.9128$, Adjusted $R^2 = 0.8381$, and Predicted $R^2 = 0.6766$. The adequate precision value was 8.6294, and the non-significant lack-of-fit confirmed the model's reliability. The fitted equation (10) was:

$$\mathbf{Y3} = 50.28 \cdot A + 42.29 \cdot B + 90.49 \cdot C + 141.42 \cdot AB + 29.17 \cdot AC + 42.09 \cdot BC \text{----------} (10)$$

PG (C), was found to have the most pronounced effect on Rel_{30} by plasticizing the film matrix, improving hydration, and facilitating drug diffusion. [51] HPMC E-15 (A) owing to its low molecular weight improves Rel_{30} by forming a hydrated diffusion matrix that controls water uptake of DLX. [52] Likewise, MD (B) enhanced rapid film wetting and dissolution due to its high-water solubility, the same result reported previously by Cupone et.al. (2022). [53] The AB interaction had the positive effect, indicating that simultaneous increases in **A** and **B** significantly enhance Rel_{30}. Interestingly, the AC interaction had a positive effect (coefficient 29.17), suggesting that increased polymer content combined with a moderate plasticizer (**C**) level enhances dissolution. The surface plots in **Figure 5** indicate that *in vitro* drug release increases with higher levels of PG that is likely to enhance matrix hydration and therefore the dissolution.

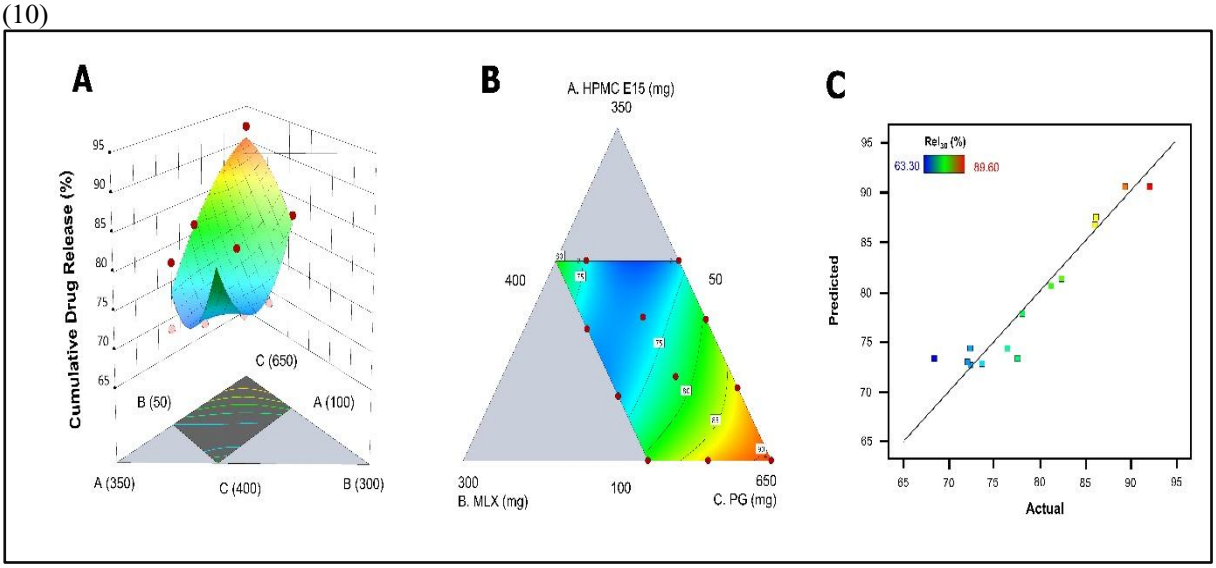

Figure 5. Three-dimensional surface plots (A), Two-dimensional contour plots (B), and Correlation plots of actual versus predicted values (C) depicting the interactive effects of independent variables on the Rel_{30} of films. The plots are color-coded, with blue indicating lower values while red indicating higher response values.

Optimization of formulation

A desirability-based numerical optimization successfully identified an optimal ODF formulation with target improved CQAs as presented in **Table 5**. The optimized film (N15) was subsequently prepared and experimentally evaluated to determine the thickness (Y_1), DT (Y_2), and Rel_{30} (Y_3), which closely aligned with the predicted values summarized in **Table 6**

.

Table 5. Results of regression analysis and polynomial coefficients about each critical parameter attribute (CPAs)

Responses	*p*-Value	R^2	Adjusted R^2
Y_1(mm)	<0.0015	0.9983	0.9972
Y_2 (s)	<0.0061	0.9909	0.9852
Y_3(%)	<0.0021	0.9128	0.8381

Table 6. Composition of the optimized formulations and comparison of the experimental values of the response parameters/product quality attributes with the predicted values.

Run	Optimal settings A: B: C	Responses	Experimental value	Predicted value	Prediction error (%)
N15**	**A**:109.43mg	Y_1(mm)	0.263±0.013	0.257	2.33
	B:53.23mg	Y_2(sec.)	27.61±2.52	27.03	2.10
	C:637.34mg	Y_3(%)	91.18±1.11	89.86	2.30

***Optimized batch (N15)*

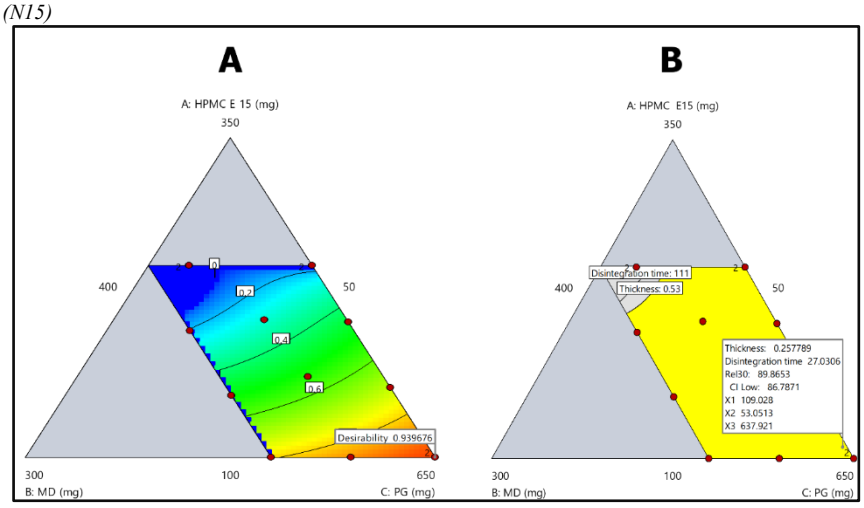

Figure 6. Plot displays the desirability response surface determined by numerical optimisation (A), with blue indicating low desirability and red indicating regions of high desirability, and the overlay design space plot (B), where the yellow region denotes the optimal formulation area, and the grey region represents conditions outside the design space, based on variations in Maltodextrin (MD), HPMC E15, and Propylene Glycol (PG) concentration.

A higher desirability value reflects stronger predictive reliability within the optimization process (**Figure 6**). For the selected optimized formulation, the prediction errors for thickness, DT, and Rel_{30} were 2.33%, 2.10%, and 2.30%, respectively, when comparing the experimental results (0.263mm, 27.61s, and 91.18%) with the corresponding predicted values (0.257mm, 27.03s, and 89.86%). These small deviations (< 5%) indicate that the developed polynomial regression models were accurate and dependable. The statistical analyses, including multiple regression analysis and ANOVA, improved the predictive strength of the constructed models. The experimentally obtained Rel_{30} and DT values for N15 closely corresponded with the predicted model responses, thereby validating the mathematical models generated. The improved dissolution behaviour of the optimized ODFs may be attributed to the highly porous hydrophilic matrix, which is likely to increase the exposed surface area and facilitate rapid disintegration and subsequent dissolution.

Compatibility studies

FTIR analysis was carried out to study the compatibility between DLX and the excipients. The spectrum of pure DLX exhibited distinct absorption bands at 3305.14 cm^{-1} (NH stretching), 1452.60 cm^{-1} (aromatic C=C stretching), 1215.87 cm^{-1} (C–N stretching), 1578.45 cm^{-1} (aromatic ring vibration), and 1236.15 cm^{-1} (C–O stretching). These characteristic peaks were also present in the physical mixture and in the optimized formulation N15, with only minor shifts observed for N15 at 3300cm^{-1} (NH stretching), 1450.23cm^{-1} (aromatic C=C stretching), 1219.02cm^{-1} (C–N stretching), 1575 cm^{-1} (C_6H_5 aromatic ring vibration), and 1236.02 cm^{-1}(C–O stretching). The retention of all major functional group peaks without significant changes confirms the compatibility of DLX with the excipients and indicates that the drug's chemical integrity remained intact, as mentioned in **Table 7**. [54]

Table 7. Fourier transform infrared characteristics and a vibrational band of Duloxetine hydrochloride, physical mixture, and oral fast dissolving film (N15)

Functional Group	Wavelength (cm^{-1})			
	Reported Wavenumber	Pure Duloxetine	Physical Mixture	Optimized Film N15
NH (Stretching)	3000–3600	3305.14	2782.78	3300
Ar C=C	1350–1500	1452.60	134.77	1450.23
C–N (Stretching)	1180–1360	1215.87	–	1219.02
C_6H_5(Aromatic Ring)	1579.05	1578.45	1317.73	1575
C–O (Bond Stretching)	1233.53	1236.15	1021.12	1236.02

Scanning Electron Microscopy

The surface morphology and topography of the optimized ODF (N15), as observed through SEM and presented in (**Figure 7**), displayed a smooth and uniform surface. This appearance reflects efficient film formation, consistent amorphous or molecular-level drug dispersion, and good excipient compatibility. These characteristics verify the robustness of the formulation method and contribute to rapid disintegration and desirable mechanical properties. [55] A smooth surface profile is particularly advantageous for ODFs, promoting patient comfort and ensuring effective drug release. [56]

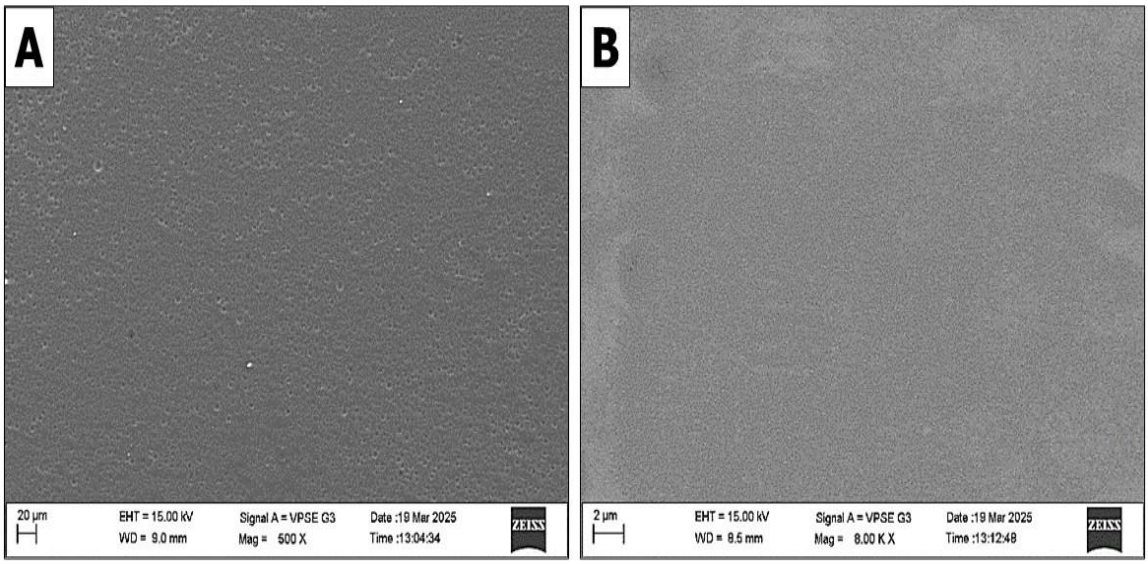

Figure 7. Scanning Electron Microscopic Analysis of Duloxetine Loaded Oral Fast-Dissolving Films: Surface Morphology at 20µm (A) and 2µm (B) magnification, respectively, of optimized film formulation (N15).

Differential Scanning Calorimetry

The DSC thermograms of pure DLX, the physical mixture, and the optimized N15 formulation reveal notable differences in thermal characteristics that reflect changes in the physical state of the drug. Pure DLX displayed a distinct and sharp endothermic melting peak at 173°C, with an onset at 169.37°C and an end set at 177.94°C, along with a high enthalpy value of −136.74 J/g, confirming its crystalline nature. In the N15, physical mixture, the DLX melting peak was still evident at 174.60°C but appeared broader and less intense, accompanied by a markedly lower enthalpy of −34.48 mJ, suggesting partial reduction in crystallinity due to simple mixing with lipid components. In comparison, the optimized N15 formulation exhibited a broad primary endothermic transition at 173.27°C with a pronounced change in heat flow −741.98 mJ, along with a minor secondary endothermic event at 187.13 °C (**Figure 8A**). The broadening and modification of the melting behavior in the optimized formulation indicate substantial disruption of the crystalline structure of DLX and its improved incorporation within the lipid matrix, supporting successful formulation development. [57,58] The amorphization of DLX in the formulation is favorable for enhancing its solubility and bioavailability.

X-ray powder diffraction

The X-ray diffraction (XRD) analysis presented above offers insight into the crystallinity and physical state of DLX, HPMC E15, MD, and their physical mixture (PM). The distinct and sharp peaks observed in the DLX spectrum, particularly around 2θ values of 19.02°, 22.84°, 24.72°, and 28.35°, confirm its highly crystalline nature (**Figure 8B**). [59] PM displayed a reduction in peak intensity and sharpness compared to pure DLX, suggesting a partial reduction in crystallinity due to interaction or dispersion within the polymer matrix. The XRD pattern of the optimized film formulation displayed a further decrease in peak intensity and the absence of sharp crystalline peaks of DLX, which confirms the conversion of DLX from a crystalline to an amorphous form. [60] This transformation is advantageous as it implies improved solubility that could potentially enhance the bioavailability of the final formulation.

***In vitro* drug release and release kinetics**

The Rel_{30} ODFs, as depicted in **Figure 8C** (**I & II**), revealed an initial rapid drug release followed by a steady release phase across all formulations. This behaviour can be attributed to efficient hydration and progressive erosion of the hydrophilic polymer–plasticizer matrix. Among the tested batches, the optimized formulation N15, containing reduced concentrations of HPMC E15 and MD along with an increased level of PG, demonstrated an appropriate balance between rapid disintegration and sufficient mechanical stability. The experimentally obtained Rel_{30} and DT values for N15 closely corresponded with the predicted model responses, thereby validating the mathematical models generated. Additionally, formulation N15 exhibited a Rel_{30} of 91.18±1.11% and a DE of 64.38±2.12%, indicating superior dissolution performance. This enhanced release behaviour may be attributed to the porous architecture of the hydrophilic matrix, which increases the effective surface area and facilitates faster film disintegration and subsequent drug dissolution.

The results of data fitment of the *in vitro* dissolution data of the ODFs are indicated in **Table 8**. Most of ODFs we found to follow first order kinetics as the dissolution rate dropped with decrease in the drug levels in the films. The mechanism of drug release was found to be dissolution as the data was found to fit well with Hixson–Crowell model. The drug release profile of the optimized batch (N15) exhibited strong agreement with both first-order kinetic behaviour and the Hixson-Crowell cube-root model, indicating the involvement of multiple release mechanisms. The release followed a concentration-dependent pattern accompanied by progressive changes in film geometry during dissolution. The optimized formulation (N15) followed both first-order ($R^2 = 0.970 \pm 0.022$) and Hixson–Crowell kinetics ($R^2 = 0.946 \pm 0.011$), indicating combined concentration-dependent dissolution and matrix erosion mechanisms. The first-order fit suggests drug release governed by the remaining DLX within the hydrophilic film, while the Hixson–Crowell rate constant ($KHC = 0.080 \pm 0.013$ μg/cm²·min$^{-1/2}$) confirms progressive surface erosion and dimensional reduction. This balanced release behaviour supports rapid and efficient duloxetine delivery. [61.

***Ex vivo* mucoadhesive and permeation studies**

The optimized ODFs (N15) displayed a strong mucoadhesive strength of 15.00±0.27g/cm^2, which can enable retention of the film in the buccal cavity until disintegration. [62] Mucoadhesion is governed by polymer properties such as hydrophilicity and molecular weight. [63] In this study, adequate mucoadhesion was found to be imparted by HPMC E15, which is known to strongly interact with mucin by hydrogen bonding and chain entanglement. [64]

Ex vivo permeation studies using goat buccal mucosa demonstrated that the film delivered 97.56±7.45μg/cm^2 of DLX within 30 min, which was comparable ($p<0.05$) to the solution form (116.77±10.68 μg/cm^2, as depicted in **Figure 8C (III & IV)**. The film exhibited comparable permeation compared to the solution, most likely due to the time taken for the film to disintegrate. The ODFs are likely to bypass the first pass effect as they would be well retained in the buccal cavity. In case the drug gets absorbed through the oral route, the pulsed release is likely to evade the gut metabolism of DLX. The *ex vivo* studies suggest the potential of the DLX-loaded ODFs to overcome the limitations of DLX and enable a prompt drug delivery to address the clinical need.

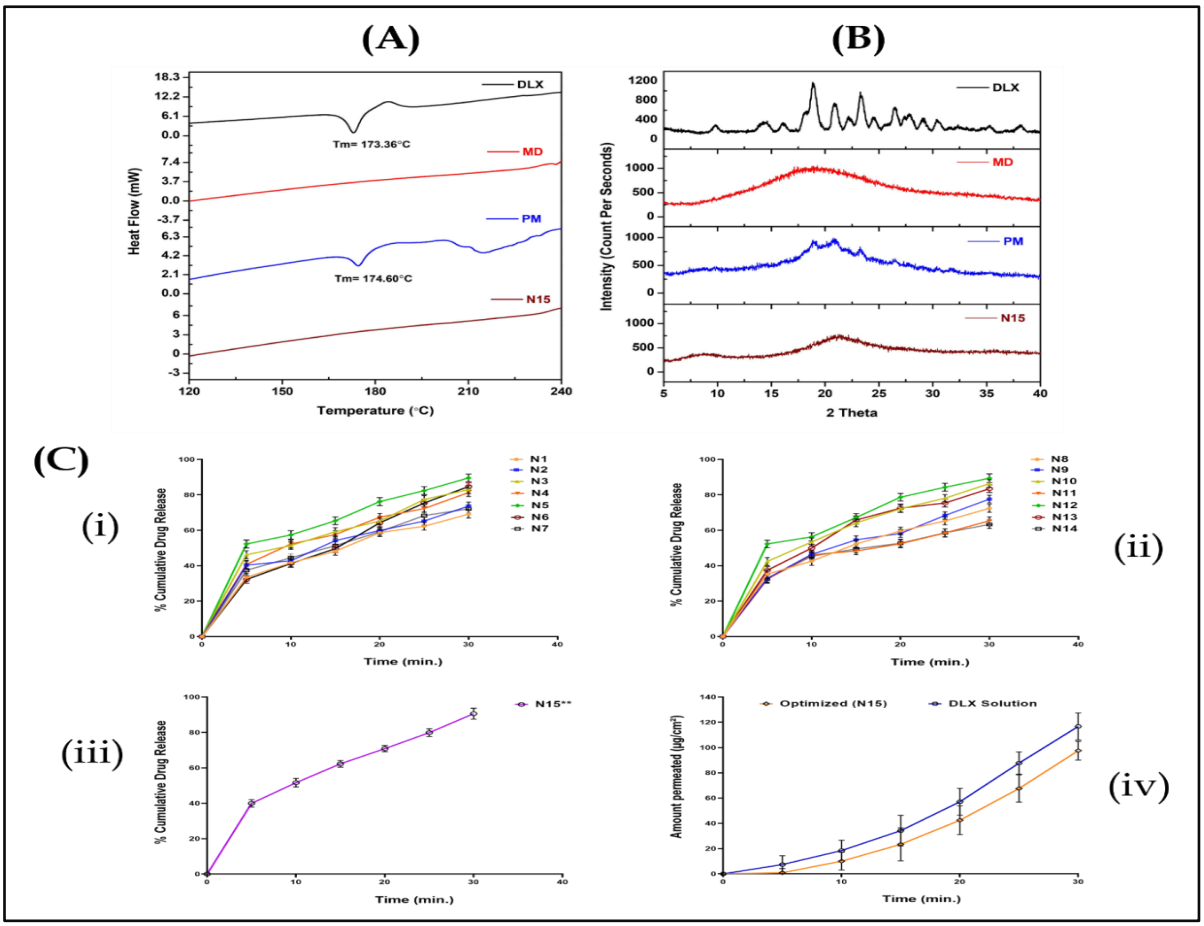

Figure 8. Differential Scanning Calorimetry (A) and X-ray diffraction patterns (B) of Duloxetine hydrochloride (DLX), Maltodextrin (MD), physical mixture (PM), and optimized film N15. *In vitro* drug release studies (C) of the film N1–N7 (i), N8–N14 (ii), and optimized formulation-N15 (iii) using the USP type-V dissolution apparatus. *Ex vivo* permeation data of optimized batch (N15) and DLX solution (iv) at 37±0.5°C. data are presented as mean±SD (n=3).**

Table 8. Curve Fitting Results of *in vitro* Dissolution Data for the Duloxetine oral fast dissolving films using various Kinetic Models.

Runs	First-order Plot		Hixon-Crowell's Plot	
	[a]K_1	R^2	[b]K_{HC}	R^2
N1	0.0362±0.003	0.964±0.002	0.050±0.017	0.941±0.021
N2	0.0356±0.014	0.947±0.010	0.056±0.012	0.921±0.038
N3	0.0347±0.025	0.955±0.012	0.069±0.011	0.933±0.012
N4	0.0349±0.007	0.966±0.043	0.066±0.021	0.942±0.024
N5	0.0341±0.021	0.963±0.041	0.082±0.032	0.939±0.025
N6	0.0346±0.055	0.967±0.005	0.072±0.011	0.982±0.010
N7	0.0358±0.046	0.948±0.015	0.054±0.014	0.924±0.011
N8	0.0358±0.004	0.970±0.018	0.054±0.014	0.947±0.043
N9	0.0353±0.004	0.897±0.048	0.061±0.012	0.918±0.038
N10	0.0344±0.021	0.980±0.038	0.075±0.021	0.961±0.027
N11	0.0367±0.045	0.916±0.041	0.046±0.013	0.888±0.022
N12	0.0342±0.046	0.974±0.024	0.082±0.025	0.944±0.035
N13	0.0347±0.021	0.979±0.022	0.070±0.012	0.955±0.027
N14	0.0370±0.052	0.906±0.040	0.042±0.011	0.876±0.011
N15**	0.0341±0.046	0.970±0.022	0.084±0.013	0.946±0.011

**Optimized batch (N15), [a]first-order release rate constant (min^{-1}), and [b]Hixson-Crowell's release rate constant ($\mu g/cm^2.min^{-1/2}$). All data in the table are represented as mean±SD (n=3)

.

CONCLUSION

Oral fast-dissolving films of duloxetine hydrochloride were successfully developed and optimized using D-optimal design integrated with FMEA-based risk assessment. The QbD assisted formulation development approach successfully produced ODFs by solvent casting method. The ODFs developed were found to possess the most desirable quality attributes, such as rapid disintegration and quick dissolution. The films that readily dissolve in the oral cavity are likely to elicit rapid onset and enable effective management of CNS disorders. Importantly, The ODFs are likely to protect DLX from acid degradation in the bioavailability. Overall, the developed ODFs platform represents a patient-friendly and effective alternative for management of CNS disorders with strong potential for further clinical translation and scale-up. However, the efficacy of the platform technology needs to be proven in preclinical models before further clinical investigations.

Author contribution

Conceptualization: Shivakumar H. N., Arpitha N, Monisha S M., **Software:** Monisha S M, Yadav V, Rushikesh Shinde., **Data curation:** Arpitha N, Shivakumar H. N., Monisha S M., **Formal analysis:** Monisha S.M., **Investigation:** Arpitha N., **Methodology:** Arpitha N., **Project administration:** Arpitha N., **Resources:** Arpitha N, Shivakumar H. N., **Validation:** Shivakumar H.N., **Visualization:** Monisha S.M., Rushikesh Shinde, Kokila S, Yadav V, Yashwanth S., **Supervision:** Shivakumar H. N., **Writing-original draft:** Monisha S.M., Yadav V., **Writing-review & editing:** Monisha S.M., Rushikesh Shinde, Kokila S, Yashwanth S., All authors have read and agreed to the published version of the manuscript.

Conflict of Interest

The author(s) declared no potential conflicts of interest with respect to the research, authorship, and/or publication of this article.

Funding

The author(s) received no financial support for the research, authorship, and/or publication of this article

REFERENCE

1. Struijs SY, de Jong PJ, Jeronimus BF, van der Does W, Riese H, Spinhoven P. Psychological risk factors and the course of depression and anxiety disorders: A review of 15 years of NESDA research. Journal of Affective Disorders. 2021 Dec 1;295:1347-59. https://doi.org/10.1016/j.jad.2021.08.086.
2. Clack S, Ward T. The classification and explanation of depression. Behaviour Change. 2019 Apr;36(1):41-55. DOI: https://doi.org/10.1017/bec.2019.4.
3. Ogbo FA, Mathsyaraja S, Koti RK, Perz J, Page A. The burden of depressive disorders in South Asia, 1990–2016: findings from the global burden of disease study. BMC psychiatry. 2018 Oct16;18(1):333. https://doi.org/10.1186/s12888-018-1918-1.
4. Dobrek L, Głowacka K. Depression and its phytopharmacotherapy—a narrative review. International Journal of Molecular Sciences. 2023 Mar 1;24(5):4772. https://doi.org/10.3390/ijms24054772
5. Paljärvi T, Tiihonen J, Lähteenvuo M, Tanskanen A, Fazel S, Taipale H. Psychotic depression and deaths due to suicide. Journal of affective disorders. 2023 Jan 15;321:28-32. https://doi.org/10.1016/j.jad.2022.10.035
6. El Sharawy AM, Shukr MH, Elshafeey AH. Formulation and optimization of duloxetine hydrochloride buccal films: in vitro and in vivo evaluation. Drug delivery. 2017 Jan 1;24(1):1762-9. https://doi.org/10.1080/10717544.2017.1402216
7. Knadler, M.P., Lobo, E., Chappell, J. et al. Duloxetine. Clin Pharmacokinet 50, 281–294 (2011). https://doi.org/10.2165/11539240-000000000-00000.
8. Shivakumar HN, Kamath M, Kumar A, Prakash S, Shinde R, Tekade A. Formulation and optimization of cilnidipine solid dispersion-based sublingual films using D-optimal mixture design. Particulate Science and Technology. 2026;44(1):111-124. https://doi.org/10.1080/02726351.2025.2576602.
9. Tekade A, Kadam P, Jagdale S, Surwade S, Gaikwad A, Pawar P, Shinde R. Exploring Potential of Nano-formulations in the Treatment of Alzheimer's Disease through Nasal Route. Curr Alzheimer Res. 2024;21(10):693-709. https://doi.org/10.2174/0115672050290462240222092303.
10. Singh A, Bali A. Formulation and characterization of transdermal patches for controlled delivery of duloxetine hydrochloride. Journal of Analytical Science & Technology. 2016;7(1)-25. https://doi.org/10.1186/s40543-016-0105-6
11. Biswajit BA, Mankad A, Dutta A. Methylphenidate fast dissolving films: development, optimization using simplex centroid design and in vitro characterization. Turkish journal of pharmaceutical sciences. 2022 Jun 27;19(3):251.doi: 10.4274/tjps.galenos.2021.99223
12. Ahmed, J. (Ed.). 2017. Glass transition and phase transitions in food and biological materials. John Wiley & Sons. doi:10.1002/9781118935682
13. Nanjappa SH, Somasekhar V, Kamath M, Prakash SS, Kumar A, Pai R, Shinde R. Formulation and evaluation of isosorbide dinitrate-loaded flash-release dispersible sublingual wafers. RSC Pharmaceutics. 2026;3:461-476. https://doi.org/10.1039/D5PM00274E.
14. Cilurzo F, Cupone IE, Minghetti P, Selmin F, Montanari L. Fast dissolving films made of maltodextrins. Eur J Pharm Biopharm. 2008 Nov;70(3):895-900. doi: 10.1016/j.ejpb.2008.06.032.
15. Zhang J, Guo M, Luo M, Cai T. Advances in the

development of amorphous solid dispersions: The role of polymeric carriers. Asian journal of pharmaceutical sciences. 2023 Jul 1;18(4):100834. doi: https://doi.org/10.1016/j.ajps.2023.100834
16. Cupone IE, Sansone A, Marra F, Giori AM, Jannini EA. Orodispersible film (ODF) platform based on maltodextrin for therapeutical applications. Pharmaceutics. 2022 Sep 22;14(10):2011. Doi: https://doi.org/10.3390/pharmaceutics14102011
17. Agarwal B, Jagdale S, Kanakdande T, Shinde RS. Nepafenac Loaded Emulgel for Controlled Ocular Delivery: In vitro and Ex vivo Characterization. *Indian J Pharm Educ Res*. 2025;59(3s):s849-s862. https://doi.org/10.5530/ijper.20251113.
18. Arya A, Chandra A, Sharma V, Pathak K. Fast dissolving oral films: an innovative drug delivery system and dosage form. Int J ChemTech Res. 2010 Jan 1;2(1):576-83.
19. Peh KK, Wong CF. Polymeric films as vehicle for buccal delivery: swelling, mechanical, and bioadhesive properties. J Pharm Pharm Sci. 1999 Aug;2(2):53-61.
20. Rowe RC, Sheskey PJ, Quinn ME. Handbook of pharmaceutical excipient. pharmaceutical press and americanpharmacists association; 2009.
21. Chougule, K.; Dandagi, P.M.; Hulyalkar, S. 2023. Esomeprazole-loaded flash release sublingual wafers: Formulation, optimization, and characterization. Journal of Pharmaceutical Innovation 18(4):2013–2028. doi:10.1007/s12247-023-09768-9.
22. Borges, A.F.; Silva, C.; Coelho, J.F.J.; Simoes, S. 2015. Oral films: Current status and future perspectives: I—Galenical development and quality attributes. Journal of Controlled Release 206:1–19. doi:10.1016/j.jconrel.2015.03.006.
23. Yasir DM, Majhi SA, Verma M, Chauhan I. Revolution of cosmetics: Cosmeceuticals. In: Recent Advances in Cosmetic Technology. Bentham Science Publishers 2025; pp. 98-121.
24. Janigová N, Elbl J, Pavloková S, Gajdziok J. Effects of various drying times on the properties of 3D printed orodispersible films. Pharmaceutics. 2022 Jan 21;14(2):250.doi: https://doi.org/10.3390/pharmaceutics14020250
25. Zaki RM, Alfadhel M, Seshadri VD, Albagami F, Alrobaian M, Tawati SM, Warsi MH, Almurshedi AS. Fabrication and characterization of orodispersible films loaded with solid dispersion to enhance Rosuvastatin calcium bioavailability. Saudi Pharmaceutical Journal. 2023 Jan 1;31(1):135-46.doi: https://doi.org/10.1016/j.jsps.2022.11.012
26. Schittny, A., Huwyler, J., & Puchkov, M. (2020). Mechanisms of increased bioavailability through amorphous solid dispersions: a review. Drug Delivery, 27(1), 110–127. https://doi.org/10.1080/10717544.2019.1704940.
27. Wali D, Nanjappa SH, Kumar A, Shinde R. Development and Optimisation of Docetaxel-Loaded Polymeric Nanoparticles for Oral Chemotherapy in Breast Cancer. Sci Pharm. 2025;93(4):58. https://doi.org/10.3390/scipharm93040058.
28. Cupone IE, Sansone A, Marra F, Giori AM, Jannini EA. Orodispersible film (ODF) platform based on maltodextrin for therapeutical applications. Pharmaceutics. 2022 Sep 22;14(10):2011.https://doi.org/10.3390/pharmaceutics14102011.
29. Imtiaz, M. M., Rashid, S. A., Naseem, F., Khan, N. R., Ullah, K., Khan, M. K., … Azad, A. K. (2025). Polymeric oral fast dissolving films of metformin: fabrication, optimization, in vitro, and in vivo evaluation. Drug Development and Industrial Pharmacy, 1–14. https://doi.org/10.1080/03639045.2025.2592675.
30. Shivakumar HN, Samreen A, Kumar A, Shinde RS. Development and Characterization of Sustained Release Solid Dispersions of Chlorzoxazone. Indian Journal of Pharmaceutical Education and Research. 2026;60(2s):s462-s474. https://doi.org/10.5530/ijper.20263331.
31. Novakovic, D.; Peltonen, L.; Isomäki, A.; Fraser-Miller, S.J.; Nielsen, L.H.; Laaksonen, T.; et al. 2020. Surface stabilization and dissolution rate improvement of amorphous compacts with thin polymer coatings: Can we have it all? Molecular Pharmaceutics 17(4):1248–1260.https://doi.org/10.1021/acs.molpharmaceut.9b01263
32. Anand, K.; Mandal, P.; Karmakar, S.; Bhowmik, R.; Shaharyar, M.A.; Mandal, A.; et al. 2024. Evaluation of cilnidipine-loaded self-micro-emulsifying drug delivery system (SMEDDS) by quantification of comparative pharmacokinetic parameters using validated LC-ESI-MS/MS bioanalytical method and pharmacodynamic assessment. Annales PharmaceutiquesFrançaises 82(6):1134–1149.https://doi.org/10.1016/j.pharma.2024.07.007
33. Dindigala AK, Anitha P, Makineni A, Viswanath V. A review on amorphous solid dispersions for improving physical stability and dissolution: Role of polymers.https://doi.org/10.30574/gscarr.2024.19.3.0231
34. Pattnaik, S., Swain, K. Techniques in the characterization of lipid-based nanotherapeutics: state of the art, challenges, and future direction. Discov. Pharm. Sci. 1, 15 (2025). https://doi.org/10.1007/s44395-025-00021-5.
35. Leonardi, D., Barrera, M.G., Lamas, M.C. et al. Development of prednisone: Polyethylene glycol 6000 fast-release tablets from solid dispersions: Solid-state

characterization, dissolution behavior, and formulation parameters. AAPS PharmSciTech 8, 108 (2007). https://doi.org/10.1208/pt0804108.
36. Brako F, Boateng J. Transmucosal drug delivery: prospects, challenges, advances, and future directions. Expert Opinion on Drug Delivery. 2025 Apr 3;22(4):525-53. https://doi.org/10.1080/17425247.2025.2470224.
37. Shin, J.-H.; Han, J.-A. Influence of Casting Variables on Release Kinetics of Orally Disintegrating Film. Foods 2024, 13, 1418. https://doi.org/10.3390/foods13091418.
38. Shivakumar HN, Kamath M, Kumar A, Prakash S, Shinde R, Tekade A. Formulation and optimization of cilnidipine solid dispersion-based sublingual films using D-optimal mixture design. Particulate Science and Technology. 2025 Oct 25:1-4. https://doi.org/10.1080/02726351.2025.2576602.
39. Gurny R. Bioadhesive intraoral release systems. In Polymeric Biomaterials 1986 May 31 (pp. 212-220). Dordrecht: Springer Netherlands. https://doi.org/10.1007/978-94-009-4390-2_13.
40. Priyanshi J, Ashish G, Gajanan D. A Detailed Overview on Mouth Dissolving Film. Journal of Drug Delivery & Therapeutics. 2023 Jul 1;13(7):172-6. http://dx.doi.org/10.22270/jddt.v13i7.6121.
41. Samal L, Prusty A. Development And Validation OfUv-Visible Spectrophotometric Method For Determination Of Duloxetine. International Journal of Pharmacy and Pharmaceutical Sciences. 2019 Jan 22;27–31. DOI: http://dx.doi.org/10.22159/ijpps.2019v11i3.30981.
42. Tekade A, Ratnaparkhi M, Shewale A, Shinde R, Kulkarni G, Pawar P. Design and assessment of in-situ nasal gel incorporated with nanostructured cubosomes for the targeted therapy of schizophrenia. *J Res Pharm*. 2025;29(3):947-
958. https://doi.org/10.12991/jrespharm.1693796.
https://doi.org/10.3390/pharmaceutics14122687
43. Singh A, Bali A. Formulation and characterization of transdermal patches for controlled delivery of duloxetine hydrochloride. Journal of Analytical Science & Technology. 2016 Nov 28;7(1).https://doi.org/10.1186/s40543-016-0105-6.
44. Krishnamoorthy B, Habibur Rahman SM, Tamil Selvan N, Hari Prasad R, Rajkumar M, Siva Selvakumar M, Vamshikrishna K, Gregory M, Vijayaraghavan C. Design, formulation, in vitro, in vivo, and pharmacokinetic evaluation of nisoldipine-loaded self-nanoemulsifying drug delivery system. Journal of Nanoparticle Research. 2015 Jan;17(1):34. https://doi.org/10.1007/s11051-014-2818-z.
45. Shivakumar HN, Shinde R, Somasekhar V, Hariprasad MG, Mahesh NM. Activation-modulated stimuli-responsive systems: an intelligent platform for site-specific gastroretentive delivery of diverse therapeutic agents. *Int J Pharm*. 2026;691:126599. https://doi.org/10.1016/j.ijpharm.2026.126599.
46. Alhamhoom Y, Sharma A, Nanjappa SH, Kumar A, Alshishani A, Ahmed MM, et al. Development and evaluation of Solid Dispersion-Based sublingual films of Nisoldipine. Pharmaceuticals. 2023 Nov 9;16(11):1589. https://doi.org/10.3390/ph16111589
47. Mushtaque M, Muhammad IN, Hassan SM, Ali A, Masood R. Development and pharmaceutical evaluation of oral fast dissolving thin film of escitalopram: A patient friendly dosage form. Pakistan journal of pharmaceutical sciences. 2020 Jan 1;33(1). https://doi.org/10.36721/PJPS.2020.33.1.REG.183-189.1.
48. Bala R, Pawar P, Khanna S, Arora S. Orally dissolving strips: A new approach to oral drug delivery system. International journal of pharmaceutical investigation. 2013 Apr;3(2):67.doi: 10.4103/2230-973X.114897
49. Irfan M, Rabel S, Bukhtar Q, Qadir MI, Jabeen F, Khan A. Orally disintegrating films: A modern expansion in drug delivery system. Saudi pharmaceutical journal. 2016 Sep 1;24(5):537-46. Doi: https://doi.org/10.1016/j.jsps.2015.02.024
50. Patel SK, Patel NJ, Patel KM, Patel PU, Patel BH. Estimation of duloxetine hydrochloride in pharmaceutical formulations by RP-HPLC method. Indian journal of pharmaceutical sciences. 2008 Nov;70(6):825. doi: 10.4103/0250-474X.49136
51. Moreira Lana G, Zhang X, Müller C, Hensel R, Arzt E. Film- Terminated fibrillar microstructures with improved adhesion on Skin-like surfaces. ACS Applied Materials & Interfaces. 2022 Oct 4;14(41):46239-51. https://doi.org/10.1021/acsami.2c12663
52. Shah KA, Li G, Song L, Gao B, Huang L, Luan D, et al. Rizatriptan-Loaded Oral Fast Dissolving Films: Design and Characterizations. Pharmaceutics. 2022 Dec 1;14(12):2687.
https://doi.org/10.3390/pharmaceutics14122687
53. Mushtaque M, Muhammad IN, Hassan SM, Ali A, Masood R. Development and pharmaceutical evaluation of oral fast dissolving thin film of escitalopram: A patient friendly dosage form. Pakistan journal of pharmaceutical sciences. 2020 Jan 1;33(1). https://doi.org/10.36721/PJPS.2020.33.1.REG.183-189.1.
54. Zhang Y, Huo M, Zhou J, Zou A, Li W, Yao C, Xie S. DDSolver: an add-in program for modeling and comparison of drug dissolution profiles. The AAPS journal. 2010 Sep 2;12:263-71. https://doi.org/10.1208/s12248-010-9185-1

55. Bonsu MA, Ofori-Kwakye K, Kipo SL, Boakye-Gyasi ME, Fosu MA. Development of oral dissolvable films of diclofenac sodium for osteoarthritis using Albizia and Khaya gums as hydrophilic film formers. Journal of drug delivery. 2016 July 18;2016(1):6459280. https://doi.org/10.1155/2016/6459280

56. Nyamba I, Sombié CB, Yabré M, Zimé-Diawara H, Yaméogo J, Ouédraogo S, Lechanteur A, Semdé R, Evrard B. Pharmaceutical approaches for enhancing solubility and oral bioavailability of poorly soluble drugs. Eur J Pharm Biopharm 2024; 204: 114513. https://dx.doi.org/10.1016/j.ejpb.2024.114513

57. Sonawane P, Shinde A. Formulation and evaluation of nanoparticulate drug delivery system of benazepril HCl. Int J Sci Res Tech 2025; 2(3). https://doi.org/10.5281/zenodo.15055510

58. Aleem O, Kuchekar B, Pore Y, Late S. Effect of β-cyclodextrin and hydroxypropyl β-cyclodextrin complexation on physicochemical properties and antimicrobial activity of cefdinir. Journal of pharmaceutical and biomedical analysis. 2008 Jul 15;47(3):535-40. https://doi.org/10.1016/j.jpba.2008.02.006

59. Abd-Elal RM, Essawy AM, Salem MA, Elsayed M, Khalil MG, Abdelhakeem E, Ali NA, Tawfik MA. Formulation, optimization, in-vivo biodistribution studies and histopathological safety assessment of duloxetine HCl-loaded ultra-elastic nanovesicles for antidepressant effect after intranasal and transdermal delivery. International Journal of Pharmaceutics: X. 2023 Dec 15;6:100194.doi: https://doi.org/10.1016/j.ijpx.2023.100194

60. Patel K, Padhye S, Nagarsenker M. Duloxetine HCl lipid nanoparticles: preparation, characterization, and dosage form design. AAPS PharmSciTech. 2012 Mar;13(1):125-33. doi: 10.1208/s12249-011-9727-6.

61. Bhadbhade MM, Gao J, Rich AM, Marjo CE. Structure of racemic duloxetine hydrochloride. Structure Reports. 2023 Apr 1;79(5):488-93. Doi: https://doi.org/10.1107/S2056989023003353

62. Veiga, A., Stofella, N.C.F., Oliveira, L.J. et al. Thermal Analytical Approaches to Characterization and Compatibility Studies of Duloxetine Hydrochloride. Pharm Chem J 54, 659–666 (2020). https://doi.org/10.1007/s11094-020-02249-0.

63. Kumar R, Sinha VR, Dahiya L, Singh G, Sarwal A. Impact of cyclodextrin derivatives on systemic release of duloxetine HCl via buccal route. Drug Dev Ind Pharm. 2020 Jun;46(6):931-945. doi: 10.1080/03639045.2020.1764019

64. Song J, Xu Z, Xie L, Shen J. Recent Advances in Studying In Vitro Drug Permeation Across Mucosal Membranes. Pharmaceutics. 2025 Feb 14;17(2):256. Doi: https://doi.org/10.3390/pharmaceutics17020256.